

HYDROTHERMAL SYNTHESIS AND SINGLE-CRYSTAL X-RAY STRUCTURE REFINEMENT OF THREE BORATES: SIBIRSKITE, PARASIBIRSKITE AND PRICEITE

WEI SUN AND YA-XI HUANG

*Department of Materials Science and Engineering, College of Materials, Xiamen University,
 Xiamen 361005, People's Republic of China*

ZUCHENG LI AND YUANMING PAN

Department of Geological Sciences, University of Saskatchewan, Saskatoon, Saskatchewan S7N 5E2, Canada

JIN-XIAO MI[§]

*Department of Materials Science and Engineering, College of Materials, Xiamen University,
 Xiamen 361005, People's Republic of China*

ABSTRACT

Sibirskite, parasibirskite and priceite, synthesized in aqueous solutions at temperatures from 80 to 240°C, have been investigated by single-crystal X-ray refinements of the structure. Sibirskite and parasibirskite are dimorphs of CaHBO₃. Sibirskite at 295 K crystallizes in space group $P12_1/c1$ (no. 14), with a 3.5624(7), b 9.5225(19), c 8.6231(17) Å, β 119.452(3)°, V 254.72(9) Å³, and $Z = 4$. Parasibirskite at 295 K crystallizes in space group $P12_1/m1$ (no. 11), with a 6.6994(13), b 5.4269(11), c 3.5534(7) Å, β 93.048(11)°, V 129.01(5) Å³, and $Z = 2$. Priceite, (Ca₂(H₂O)[B₅O₇(OH)₅]), at 173 K crystallizes in space group of $P12_1/c1$ (no. 14), with a 11.580(3), b 6.9844(19), c 12.352(3) Å, β 110.573(9)°, V 935.3(4) Å³, and $Z = 4$. Our refinements allow determination of the positions of boron and hydrogen atoms in these minerals, which was not possible in previous powder XRD studies. In particular, the isolated [BO₂(OH)] groups in sibirskite and parasibirskite are characterized by a long B–OH bond and two short B–O bonds, different from the [BO₃] and [B(OH)₃] groups in nesoborates. Periodic density functional theory (DFT) calculations for sibirskite and parasibirskite support those results of structure refinements and suggest that parasibirskite undergoes a displacive phase-transition involving hydrogen ordering below 173 K. Sibirskite and parasibirskite left in their parental solutions at ambient conditions decompose to form calcite.

Keywords: sibirskite, parasibirskite, priceite, hydrothermal synthesis, single-crystal X-ray structure refinements, DFT calculations, hydrogen bonding, stability.

SOMMAIRE

Nous avons caractérisé la structure cristalline de la sibirskite, parasibirskite et priceite, synthétisées en solutions aqueuses entre 80 et 240°C, par affinement avec rayons X sur monocristaux. La sibirskite et la parasibirskite sont des dimorphes de CaHBO₃. A 295 K, la sibirskite cristallise dans le groupe spatial $P12_1/c1$ (no. 14), avec a 3.5624(7), b 9.5225(19), c 8.6231(17) Å, β 119.452(3)°, V 254.72(9) Å³, et $Z = 4$. La parasibirskite à 295 K cristallise dans le groupe spatial $P12_1/m1$ (no. 11), avec a 6.6994(13), b 5.4269(11), c 3.5534(7) Å, β 93.048(11)°, V 129.01(5) Å³, et $Z = 2$. La priceite, (Ca₂(H₂O)[B₅O₇(OH)₅]), cristallise dans le groupe spatial $P12_1/c1$ (no. 14) à 173 K, avec a 11.580(3), b 6.9844(19), c 12.352(3) Å, β 110.573(9)°, V 935.3(4) Å³, et $Z = 4$. Nos affinements permettent la détermination des positions des atomes de bore et d'hydrogène dans ces minéraux, ce qui n'avait pas été possible avec la diffraction X sur poudre. En particulier, les groupes isolés [BO₂(OH)] dans la sibirskite et la parasibirskite possèdent une longue liaison B–OH et deux liaisons B–O plus courtes, ce qui les distinguent des groupes [BO₃] et [B(OH)₃] des nésoborates. D'après les calculs de la densité fonctionnelle périodique théorique (DFT) pour la sibirskite et la parasibirskite, qui confirment les résultats des affinements structuraux, la parasibirskite montrerait une transition de phase displacive impliquant la mise en ordre des atomes d'hydrogène à une température inférieure à 173 K. Les cristaux de sibirskite et de parasibirskite, laissés dans leurs solutions aqueuses originales à température ambiante, se décomposent pour former la calcite.

[§] E-mail address: jxmi@xmu.edu.cn

Mots-clés: sibirskite, parasibirskite, priceite, synthèse hydrothermale, affinement de la structure, diffraction X sur monocristal, calculs DFT, liaisons hydrogène, stabilité.

INTRODUCTION

Alkaline-earth metal borates have long attracted considerable attention, not only for their important applications in modern technology [*e.g.*, β -BaB₂O₄ (BBO)] as nonlinear optical materials: Chen *et al.* 1985, Solntsev *et al.* 2008, Filatov & Bubnova 2008), but also for their rich structural chemistry arising from the complex polymerization of planar triangular [B ϕ ₃] and tetrahedral [B ϕ ₄] groups, where ϕ represents O²⁻ and OH⁻ (Hawthorne *et al.* 1996, Grice *et al.* 1999, Yuan & Xue 2007). For example, the diverse linkages of fundamental building blocks (FBBs) of borate polyanions give rise to at least 29 calcium borates, 20 of which are minerals. However, structural studies for several hydroxy-hydrated calcium borates are limited owing to the lack of materials for high-quality single-crystal X-ray structure refinements.

Sibirskite and parasibirskite are dimorphs of CaHBO₃. Sibirskite was first discovered in the Yuliya Svintsoviya deposit, eastern Siberia, and the Novofrolovskoye B–Cu deposit, Urals (Vasilkova 1962), and was also reported to occur in a vein along the contact between limestone and skarn at Fuka, Okayama Prefecture, Japan (Kusachi *et al.* 1997). Kusachi *et al.* (1998) established parasibirskite as a new mineral species with material from the same occurrence at Fuka, Japan. The crystal structures of sibirskite and parasibirskite have only been determined recently by using combined Monte Carlo calculations and Rietveld refinements of powder X-ray diffraction (PXRD) data (Miura & Kusachi 2008, Takahashi *et al.* 2010). Similarly, priceite, Ca₂(H₂O)[B₅O₇(OH)₅], has been known since the 1870s (Palache *et al.* 1951), but its crystal structure was solved only recently by using PXRD data (Wallwork *et al.* 2002). Because of the limitation of the PXRD method, questions remain about the crystal structures of these hydroxy-hydrated calcium borates. For example, the positions of boron and hydrogen atoms in sibirskite, parasibirskite, and priceite have not been determined in previous structural studies quoted.

As part of our research program on alkaline-earth metal borates (Sun *et al.* 2010), we have succeeded in synthesizing sibirskite, parasibirskite and priceite that are suitable for single-crystal X-ray refinements of their structure. To the best of our knowledge, this is the first-ever synthesis of sibirskite. Herein, we first describe the experimental synthesis of sibirskite, parasibirskite, and priceite. Then, we report the results of single-crystal X-ray refinements of the structure of these

three minerals, with emphasis on the determination of the boron and hydrogen positions. Also, the crystal structures of sibirskite and parasibirskite, including the hydrogen positions and hydrogen bonds, have been evaluated by first-principles calculations at the density functional theory (DFT) level.

EXPERIMENTAL DETAILS

Hydrothermal synthesis

All three calcium borates, sibirskite, parasibirskite and priceite, were synthesized by using a hydrothermal method. A typical synthesis route for growing parasibirskite is as follows. A mixture of 1.0 g LiOH•H₂O (23.83 mmol), 1.0 g H₃BO₃ (16.17 mmol) and 0.8 g Ca(OH)₂ (10.8 mmol) with a molar proportion Li:B:Ca of 4.4:3:2 was prepared. All starting reagents were of analytical grade and used without any further purification. After adding 15 mL deionized water, the mixture, with a pH value of ~14, was transferred into a 30 mL Teflon-lined stainless-steel autoclave, heated to and held at 190°C for three days, and finally cooled down to room temperature by turning off the furnace. Reconnaissance experiments show that parasibirskite can be synthesized at a wide range of conditions; for example, LiOH•H₂O can vary from 0.8 to 2.0 g, temperature from 80 to 240°C, and CaO or CaCl₂ can be used instead of Ca(OH)₂ as the source of calcium. Also, parasibirskite has been synthesized by using KOH instead of LiOH•H₂O. Therefore, the basic nature of the solution, not the presence of LiOH•H₂O, is the main factor in the formation of parasibirskite.

To synthesize sibirskite, the condition is similar to that for parasibirskite, except that 0.8 g CaCl₂ (7.21 mmol), not Ca(OH)₂ or CaO, is required as the source of calcium, the amount of water has to be decreased to 5 mL, and temperature must be kept at 190°C.

Priceite was obtained from reconnaissance experiments designed to explore the optimal conditions for the synthesis of sibirskite and parasibirskite. For example, experiments with a mixture of 1.0 g H₃BO₃ and 1.0 g CaCl₂, but no Li(OH)•H₂O, at 190°C for three days produced pure priceite (Fig. 1a). Indeed, priceite can be synthesized from a wide range of conditions in the absence of Li(OH)•H₂O: temperature from 130 to 240°C, H₂O from 5 to 20 mL, CaCl₂ or Ca(OH)₂ as the source of calcium, and the molar value of Ca/B can range from 2/3 to 3/2. However, addition of Li(OH)•H₂O to the above mixtures resulted in

the formation of both priceite and parasibirskite. The proportion of parasibirskite and priceite increases with increasing $\text{Li(OH)•H}_2\text{O}$ (Figs. 1b, c). Pure parasibirskite is obtained in the range of $\text{Li(OH)•H}_2\text{O}$ from 1.0 to 1.5 g (Fig. 1d). However, further increase in the amount of $\text{Li(OH)•H}_2\text{O}$ to 2.0 g led to the formation of pure LiCaBO_3 (Fig. 1e).

Solid products of all synthesis experiments were filtered, washed with deionized water, and dried in desiccators. Optical examination and PXRD analysis were used to identify these solid products. Scanning electron microscopy was used to document crystal morphologies (Fig. 2). Selected crystals of sibirskite, parasibirskite and priceite were also examined with an Oxford Instruments energy-dispersive spectrometer, but neither chemical zonation nor nonstoichiometric impurities were detected.

Single-crystal X-ray structure refinement

Single-crystal X-ray-diffraction datasets for sibirskite (295 K), parasibirskite (295 and 173 K), and priceite (173 K; Table 1) were all collected on a Bruker AXS CCD diffractometer (MoK α radiation, graphite monochromator, 50 kV, 40 mA, scan types: three blocks for $\phi = 0, 90, 180^\circ$, and $\Delta\omega = 0.3^\circ$, $\psi =$

54.74° , 600 frames). The raw X-ray-diffraction data were corrected for Lorentz and polarization effects. The crystal structures were solved and refined with the SHELX97 software package (Sheldrick 1997).

The positions of the hydrogen atoms in sibirskite were obtained from difference-Fourier maps and refined without applying any constraint. Two space groups ($P2_1$ and $P2_1/m$) have been evaluated during the structure refinement of parasibirskite. All atoms except hydrogen have been located in the centrosymmetric cell, whereas hydrogen atoms have been determined in the acentric cell. The centrosymmetric space-group $P2_1/m$ was favored by a search with the program PLATON (Spek 2003) and was finally selected, because its bond-distance deviations are significantly smaller than those refined from the acentric space-group $P2_1$. Hydrogen sites were refined in the disordered mode with 50% occupancies, using the constraint of $d(\text{O-H}) \approx 1.0 \text{ \AA}$ and twofold isotropic U of the linked oxygen atom.

All hydrogen positions in priceite were obtained from difference-Fourier maps as well, and fixed without any refinement. Their isotropic displacement parameters, except for H(6) and H(7) of the H_2O molecule, were refined (Table 1).

The coordinates and isotropic displacement parameters, and anisotropic displacement parameters of atoms,

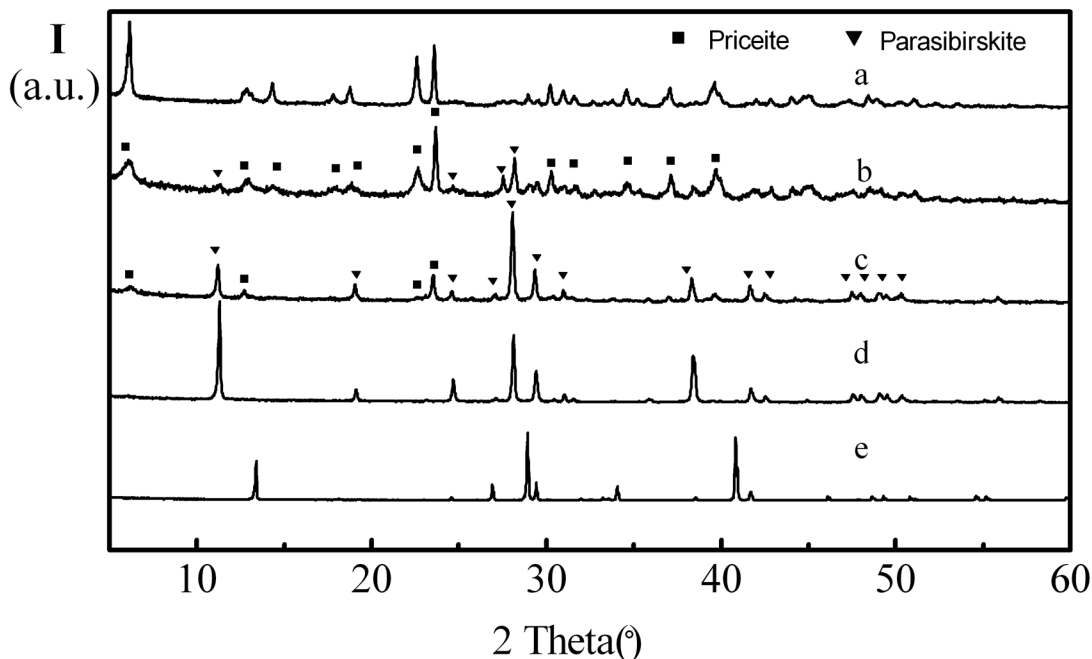


FIG. 1. Powder X-ray diffraction patterns illustrate the effect of $\text{Li(OH)•H}_2\text{O}$ on the solid products in experiments with 1.0 g H_3BO_3 and 1.0 g CaCl_2 at 190°C for 3 days: (a) pure priceite without $\text{Li(OH)•H}_2\text{O}$, (b) and (c) mixtures of priceite and parasibirskite with addition of 0.4 g and 0.6 g $\text{Li(OH)•H}_2\text{O}$, respectively, (d) pure parasibirskite with 1.0 g $\text{Li(OH)•H}_2\text{O}$, and (e) pure LiCaBO_3 using 2.0 g $\text{Li(OH)•H}_2\text{O}$.

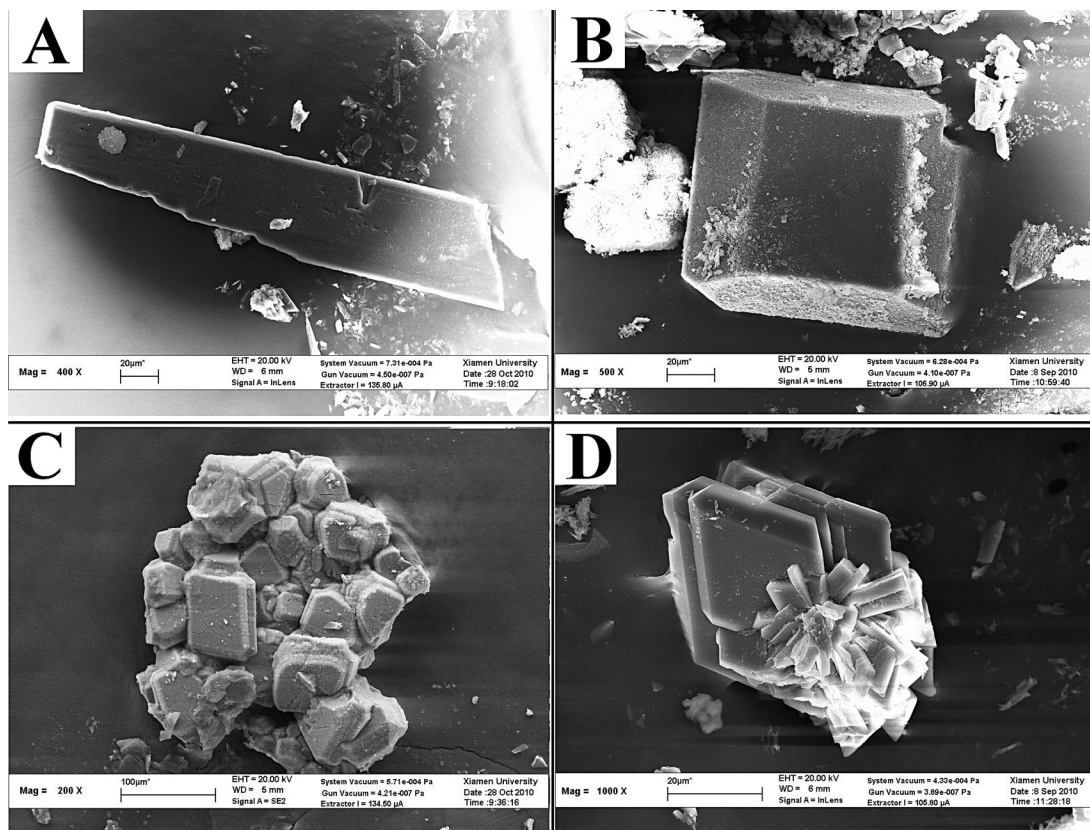


FIG. 2. Scanning electron microscope images of (A) sibirskite, (B) parasibirskite, (C) calcite formed from the decomposition of parasibirskite, and (D) priceite.

as well as selected interatomic distances and angles of the three borates, are listed in Tables 2 to 6. Further details of these crystal-structure investigations are available from the Fachinformationszentrum Karlsruhe, D-76344 Eggenstein-Leopoldshafen (Germany), on quoting the depository number CSD-422608-422611, the name of the authors, and citation of the paper. A table of structure factors and a cif file are available from the Depository of Unpublished Data on the MAC website [document Sibirskite CM49_823].

First-principles calculations

First-principles calculations have been made by use of the supercell approach and hybrid functional B3PW91 as implemented in CRYSTAL06 (Dovesi *et al.* 2006). All-electron basis sets used in this study are those known to be well suited for periodic calculations and include the 86-511D21G of Valenzano *et al.* (2006) for Ca, standard 6-31G* for O and H (Gatti *et al.* 1994), and the def2-TZVP of Weigend & Ahlrichs (2005) for

B, except that the diffuse functions with exponents < 0.1 were left out, along with the outermost *d* and *f* functions, to avoid linear correlation and integration problems in the calculations.

The thresholds for the overlap and penetration Coulomb integrals, the overlap of Hartree-Fock (HF) exchange integrals, and the two pseudo-overlaps for HF series were set to 10^{-7} , 10^{-7} , 10^{-7} , 10^{-7} , and 10^{-14} hartree, respectively, whereas a tight SCF tolerance of 10^{-7} hartree was chosen. They are all more accurate than the default values to improve the optimized crystal-structures. The Pack-Monkhorst shrink factor for the unit-cell geometry optimization was set to 8, giving a total of 170 *k* points in the irreducible Brillouin zone. The same shrink factor was also used for the Gilat net to describe the Fermi surface of the system (Dovesi *et al.* 2006). Space group $P2_1/c$ was used for sibirskite, whereas calculations for parasibirskite at 0 K were made in space group $P2_1$ (see below).

TABLE 1. CRYSTALLOGRAPHIC DATA AND STRUCTURE-REFINEMENT RESULTS FOR SIBIRSKITE, PARASIBIRSKITE, AND PRICEITE

Mineral	sibirskite (295 K)	parasibirskite (295 K)	parasibirskite (173 K)	priceite (173 K)
Crystal size (mm), colorless	0.10 × 0.09 × 0.02	0.17 × 0.12 × 0.08	0.18 × 0.11 × 0.08	0.25 × 0.12 × 0.10
Formula weight, Z	99.90, 4	99.90, 2	99.90, 2	349.27, 4
Crystal system, space group	monoclinic <i>P12₁/c1</i> (no. 14)	monoclinic <i>P12₁/m1</i> (no. 11)	monoclinic <i>P12₁/m1</i> (no. 11)	monoclinic <i>P12₁/c1</i> (no. 14)
Cell parameters				
<i>a</i> , <i>b</i> (Å)	3.5624(7), 9.5225(19)	6.6994(13), 5.4269(11)	6.6798(8), 5.4208(9)	11.580(3), 6.9844(19)
<i>c</i> , β (Å, °)	8.6231(17), 119.452(3)	3.5534(7), 93.048(11)	3.5466(4), 93.245(9)	12.352(3), 110.573(9)
Volume (Å ³), density (g/cm ³)	254.72(9), 2.605	129.01(5), 2.572	128.22(3), 2.588	935.3(4), 2.480
Radiation (Å)	0.71073 (MoKα)	0.71073 (MoKα)	0.71073 (MoKα)	0.71073 (MoKα)
μ (mm ⁻¹), <i>F</i> (000), 2θ _{max} (°)	2.190, 200, 56.46	2.162, 100, 56.40	2.176, 100, 57.24	1.300, 704, 56.62
Range, Miller indices	-4 ≤ <i>h</i> ≤ 4, -12 ≤ <i>k</i> ≤ 12, -10 ≤ <i>l</i> ≤ 11	-8 ≤ <i>h</i> ≤ 8, -6 ≤ <i>k</i> ≤ 6, -4 ≤ <i>l</i> ≤ 4	-7 ≤ <i>h</i> ≤ 8, -5 ≤ <i>k</i> ≤ 6, -3 ≤ <i>l</i> ≤ 4	-15 ≤ <i>h</i> ≤ 15, -9 ≤ <i>k</i> ≤ 9, -16 ≤ <i>l</i> ≤ 16
<i>R</i> _{int} , <i>R</i> _{σ(I)}	0.0383, 0.0408	0.0236, 0.0243	0.0348, 0.0472	0.0682, 0.0745
Goof, <i>N</i> _{param}	1.000, 50	1.000, 31	1.000, 32	1.000, 181
<i>R</i> _{gt} (no.), <i>wR</i> _{gt} (no.)	0.0342 (490), 0.0892 (599)	0.0205 (325), 0.0652 (325)	0.0216(304), 0.0601(325)	0.0513 (1626), 0.1323 (2188)
LDPH*, Pearson code	0.580, -0.577, <i>mP24</i>	0.270, -0.265, <i>mP12</i>	0.461, -0.396, <i>mP12</i>	0.764, -0.574, <i>mP108</i>
SDABD: (Ca–O), (B–O)	0.002, 0.004	0.0013, 0.002	0.0014, 0.003	0.003, 0.005

* LDPH denotes the largest difference electron-density peak / hole (e/Å³). Goof is the Goodness-of-fit and is fixed at 1.000. SDABD is the standard deviation of the average Ca–O and B–O bond distances.

TABLE 2. COORDINATES AND ISOTROPIC OR ANISOTROPIC DISPLACEMENT PARAMETERS OF ATOMS IN SIBIRSKITE AND PARASIBIRSKITE

Atom Wyckoff	<i>x/a</i>	<i>y/b</i>	<i>z/c</i>	<i>U</i> ₁₁	<i>U</i> ₂₂	<i>U</i> ₃₃	<i>U</i> ₁₂	<i>U</i> ₁₃	<i>U</i> ₂₃
Sibirskite (295 K)									
Ca(1) 4e	0.50358(18)	0.49298(6)	0.71256(8)	0.0103(3)	0.0103(3)	0.0117(4)	-0.0004(2)	0.0056(3)	-0.0005(2)
O(1) 4e	0.1641(6)	0.3794(2)	0.4262(3)	0.0129(9)	0.0087(10)	0.0111(10)	0.0005(8)	0.0055(8)	-0.0013(8)
O(2) 4e	0.1026(6)	0.1525(2)	0.2908(3)	0.0134(10)	0.0117(10)	0.0123(11)	-0.0019(8)	0.0073(8)	-0.0030(8)
O(3) 4e	0.1282(7)	0.1669(2)	0.5671(3)	0.0274(12)	0.0108(11)	0.0162(12)	0.0025(9)	0.0142(10)	0.0027(9)
B(1) 4e	0.1405(10)	0.2363(3)	0.4250(4)	0.0056(14)	0.0153(16)	0.0094(15)	-0.0002(11)	0.0035(12)	-0.0001(13)
H(1) 4e	0.093(14)	0.230(4)	0.627(6)	0.045(13)*					
Parasibirskite (295 K)									
Ca(1) 2e	0.35260(6)	1/4	0.24837(12)	0.0115(3)	0.0072(3)	0.0094(3)	0.00000	0.00105(18)	0.00000
O(1) 2e	0.0236(3)	3/4	0.8724(6)	0.0115(9)	0.0293(11)	0.0322(11)	0.00000	0.0074(8)	0.00000
O(2) 4f	0.3188(1)	0.5318(2)	0.7367(3)	0.0198(6)	0.0085(7)	0.0119(6)	-0.0002(5)	0.0026(5)	-0.0003(4)
B(1) 2e	0.2251(4)	3/4	0.7704(7)	0.0092(11)	0.0112(11)	0.0088(10)	0.00000	-0.0002(8)	0.00000
H(1)** 4f	-0.030(8)	0.863(8)	0.974(17)	0.0480					
Parasibirskite (173 K)									
Ca(1) 2e	0.35264(8)	1/4	0.24743(14)	0.0068(3)	0.0053(3)	0.0058(3)	0.00000	0.00079(18)	0.00000
O(1) 2e	0.0227(3)	3/4	0.8727(6)	0.0073(11)	0.0244(13)	0.0207(12)	0.00000	0.0037(8)	0.00000
O(2) 4f	0.3186(2)	0.5316(3)	0.7353(3)	0.0128(8)	0.0061(8)	0.0080(7)	-0.0004(5)	0.0013(5)	-0.0003(5)
B(1) 2e	0.2242(5)	3/4	0.7690(8)	0.0054(14)	0.0112(15)	0.0042(13)	0.00000	-0.0003(10)	0.00000
H(1)** 4f	-0.006(9)	0.887(6)	0.938(17)	0.0350					

* for isotropic displacement parameters; ** Hydrogen in 4f with occupancies 50%.

TABLE 3. COORDINATES AND ISOTROPIC OR ANISOTROPIC DISPLACEMENT PARAMETERS OF ATOMS IN PRICEITE

Atom	Wyckoff	<i>x/a</i>	<i>y/b</i>	<i>z/c</i>	<i>U</i> ₁₁	<i>U</i> ₂₂	<i>U</i> ₃₃	<i>U</i> ₁₂	<i>U</i> ₁₃	<i>U</i> ₂₃
Ca(1)	4e	0.00800(7)	0.75771(10)	0.57987(6)	0.0077(4)	0.0058(4)	0.0061(4)	-0.0002(3)	0.0028(3)	0.0006(3)
Ca(2)	4e	0.30866(7)	0.24418(10)	0.37863(6)	0.0085(4)	0.0064(4)	0.0062(4)	0.0001(3)	0.0030(3)	-0.0007(3)
O(1)	4e	0.3200(2)	0.7557(3)	0.7756(2)	0.0101(13)	0.0058(13)	0.0058(12)	-0.0009(10)	0.0053(10)	-0.0018(9)
O(2)	4e	0.2975(2)	0.9158(3)	0.4342(2)	0.0104(14)	0.0067(13)	0.0089(13)	-0.0003(10)	0.0028(11)	-0.0032(10)
O(3)	4e	0.2667(2)	0.5707(3)	0.4177(2)	0.0082(13)	0.0074(13)	0.0048(12)	0.0004(10)	0.0019(10)	0.0011(10)
O(4)	4e	0.1163(2)	0.7835(4)	0.2860(2)	0.0086(13)	0.0093(13)	0.0077(13)	0.0004(10)	0.0035(11)	0.0044(10)
O(5)	4e	-0.0206(2)	0.8926(4)	0.3870(2)	0.0094(14)	0.0093(13)	0.0109(13)	-0.0007(10)	0.0060(11)	0.0011(11)
O(6)	4e	-0.0907(2)	0.6732(4)	0.2256(2)	0.0076(13)	0.0066(13)	0.0068(13)	-0.0005(10)	0.0003(11)	0.001(1)
O(7)	4e	0.0546(2)	0.5652(3)	0.4098(2)	0.0107(13)	0.0049(12)	0.0068(13)	-0.0013(10)	0.0040(11)	0.0011(10)
O(8)	4e	0.2121(2)	0.6706(4)	0.5819(2)	0.0089(13)	0.0061(13)	0.0061(12)	0.0007(10)	0.0027(10)	-0.0002(10)
O(9)	4e	0.1995(2)	0.3349(3)	0.5215(2)	0.0097(13)	0.0051(13)	0.0050(12)	-0.0005(10)	0.0016(10)	0.0011(10)
O(10)	4e	0.2670(2)	0.1177(3)	0.6820(2)	0.0102(13)	0.0060(13)	0.0088(13)	0.0005(10)	0.0023(11)	0.0027(10)
O(11)	4e	0.4076(2)	0.2472(3)	0.5891(2)	0.0065(14)	0.0144(14)	0.0094(14)	0.0033(10)	0.0027(11)	0.0004(10)
O(12)	4e	0.3312(2)	0.4351(3)	0.7148(2)	0.0129(14)	0.0053(12)	0.0071(12)	0.0007(10)	0.0047(11)	0.0004(10)
OW(1)	4e	0.5087(3)	0.3473(4)	0.3950(2)	0.0129(15)	0.0268(17)	0.0183(15)	-0.0059(12)	0.0043(12)	0.0026(13)
B(1)	4e	0.2490(4)	0.7492(6)	0.3541(4)	0.005(2)	0.010(2)	0.008(2)	-0.0012(15)	0.0028(16)	-0.0026(16)
B(2)	4e	0.0181(4)	0.7255(6)	0.3284(3)	0.008(2)	0.006(2)	0.0046(19)	0.0006(15)	0.0001(16)	-0.0012(15)
B(3)	4e	0.1845(4)	0.5344(6)	0.4811(3)	0.009(2)	0.005(2)	0.007(2)	-0.0013(15)	0.0026(17)	-0.0021(15)
B(4)	4e	0.3032(4)	0.2810(6)	0.6271(3)	0.009(2)	0.009(2)	0.0025(19)	-0.0010(15)	0.0010(16)	0.0000(15)
B(5)	4e	0.2899(4)	0.6203(6)	0.6904(3)	0.0064(8)*					
H(1)	4e	0.47970	0.22620	0.63640	0.06(2)					
H(2)	4e	0.31320	0.01140	0.70630	0.035(14)					
H(3)	4e	0.25680	0.93040	0.48580	0.047(17)					
H(4)	4e	-0.10210	0.87040	0.37790	0.063(19)					
H(5)	4e	-0.10290	0.54640	0.23450	0.048(17)					
H(6)	4e	0.55430	0.26380	0.44000	0.0500					
H(7)	4e	0.53280	0.46600	0.39980	0.0500					

* for isotropic displacement parameters.

TABLE 4. SELECTED BOND-DISTANCES (Å) AND ANGLES (°) FOR SIBIRSKITE AND PARASIBIRSKITE, AND A COMPARISON WITH THOSE FROM PXRD STUDIES AND DFT CALCULATIONS

sibirskite				parasibirskite				
	295 K	PXRD*	DFT		295 K	173 K	PXRD*	DFT**
Ca(1) -- O(1)	2.388(2)	2.341(4)	2.377	Ca(1) -- O(1)	2.533(2)	2.519(2)	2.539(8)	2.516
-- O(1)	2.401(2)	2.423(4)	2.379	-- O(2) × 2	2.333(1)	2.328(1)	2.336(3)	2.323
-- O(1)	2.407(2)	2.426(8)	2.382	-- O(2) × 2	2.377(1)	2.374(1)	2.363(3)	2.398
-- O(2)	2.316(2)	2.303(4)	2.318	-- O(2) × 2	2.498(1)	2.493(1)	2.509(3)	2.437
-- O(2)	2.348(2)	2.312(5)	2.341	Average	2.421	2.415	2.422	2.404
-- O(3)	2.372(2)	2.390(5)	2.378					
Average	2.372	2.366	2.363					
B(1) -- O(1)	1.365(4)	1.389(14)	1.364	B(1) -- O(1)	1.417(3)	1.415(4)	1.350(8)	1.426
-- O(2)	1.356(4)	1.393(13)	1.363	-- O(2) × 2	1.349(1)	1.350(2)	1.395(5)	1.360
-- O(3)	1.412(4)	1.393(14)	1.416	Average	1.371	1.372	1.380	1.382
Average	1.378	1.392	1.381					
O(3) -- H	0.84(4)		1.020	O(1) -- H	0.97(2)	0.97(2)		1.031
O(1) -- B(1) -- O(2)	125.0(3)		124.6	O(1) -- B(1) -- O(2)	118.5(1)	118.6(1)		120.1
O(1) -- B(1) -- O(3)	119.2(3)		119.6	O(2) -- B(1) -- O(2)	122.8(2)	122.5(2)		122.5
O(2) -- B(1) -- O(3)	115.6(3)		115.5					

* PXRD data for sibirskite and parasibirskite from Miura & Kusachi (2008) and Takahashi *et al.* (2010), respectively; ** DFT calculation at 0 K for the space group *P2*₁.

TABLE 5. SELECTED BOND-DISTANCES (Å) AND ANGLES (°) FOR PRICEITE, AND COMPARISON WITH DATA FROM PREVIOUS PXRD STUDY

	173 K	PXRD*		173 K	PXRD*
Ca(1) --O(4)	2.428(3)	2.448(4)	B(2) --O(4)	1.466(5)	1.49
--O(5)	2.472(3)	2.452(3)	--O(5)	1.521(5)	1.50
--O(5)	2.474(3)	2.478(4)	--O(6)	1.487(5)	1.47
--O(6)	2.495(3)	2.480(4)	--O(7)	1.464(5)	1.47
--O(7)	2.386(3)	2.392(3)	Average	1.485	
--O(7)	2.703(3)	2.746(4)	B(3) --O(3)	1.451(5)	1.47
--O(8)	2.432(3)	2.488(4)	--O(7)	1.467(5)	1.49
--O(9)	2.376(3)	2.384(3)	--O(8)	1.509(5)	1.49
Average	2.471		--O(9)	1.470(5)	1.49
Ca(2) --O(2)	2.410(3)	2.394(4)	Average	1.474	
--O(3)	2.416(3)	2.414(4)	B(4) --O(9)	1.478(5)	1.46
--O(6)	2.447(3)	2.452(3)	--O(10)	1.462(5)	1.48
--O(9)	2.585(3)	2.597(4)	--O(11)	1.462(5)	1.48
--O(10)	2.498(3)	2.527(4)	--O(12)	1.480(5)	1.49
--O(11)	2.445(3)	2.466(3)	Average	1.471	
--O(12)	2.470(3)	2.490(4)	B(5) --O(1)	1.366(5)	1.36
--OW(1)	2.366(3)	2.386(4)	--O(8)	1.373(5)	1.37
Average	2.454		--O(12)	1.375(5)	1.39
B(1) --O(1)	1.476(5)	1.46	Average	1.371	
--O(2)	1.503(5)	1.49	O(3)--B(3)--O(8)	110.3(3)	
--O(3)	1.449(5)	1.48	O(7)--B(3)--O(8)	106.1(3)	
--O(4)	1.490(5)	1.49	O(9)--B(3)--O(8)	110.6(3)	
Average	1.479		O(10)--B(4)--O(9)	115.3(3)	
O(3)--B(1)--O(1)	109.4(3)		O(11)--B(4)--O(9)	109.4(3)	
O(3)--B(1)--O(4)	111.4(3)		O(10)--B(4)--O(12)	105.4(3)	
O(1)--B(1)--O(4)	109.6(3)		O(11)--B(4)--O(12)	104.6(3)	
O(3)--B(1)--O(2)	111.1(3)		O(9)--B(4)--O(12)	111.1(3)	
O(1)--B(1)--O(2)	106.6(3)		O(1)--B(5)--O(8)	111.2(3)	
O(4)--B(1)--O(2)	108.7(3)		O(1)--B(5)--O(12)	118.5(3)	
O(7)--B(2)--O(4)	112.6(3)		O(8)--B(5)--O(12)	120.5(3)	
O(7)--B(2)--O(6)	110.6(3)		B(5)--O(1)--B(1) ^f	120.9(3)	
O(4)--B(2)--O(6)	107.0(3)		B(1)--O(3)--B(3)	116.1(3)	
O(7)--B(2)--O(5)	108.8(3)		B(2)--O(4)--B(1)	116.6(3)	
O(4)--B(2)--O(5)	110.7(3)		B(2)--O(7)--B(3)	122.0(3)	
O(6)--B(2)--O(5)	107.0(3)		B(5)--O(8)--B(3)	120.8(3)	
O(3)--B(3)--O(7)	112.3(3)		B(3)--O(9)--B(4)	121.4(3)	
O(3)--B(3)--O(9)	109.1(3)		B(5)--O(12)--B(4)	120.3(3)	
O(7)--B(3)--O(9)	108.4(3)				

* PXRD data from Wallwork *et al.* (2002).

RESULTS AND DISCUSSION

The crystal structure of sibirskite

In the original definition of sibirskite, Vasilkova (1962) did not determine its space group. Miura & Kusachi (2008) adopted the non-standard space-group $P2_1/a$ for their PXRD analysis of sibirskite. In this study, we opted for the standard space-group $P2_1/c$ (Table 1). The crystal structure of sibirskite can be envisaged as double chains of [CaO₆] octahedra linked together by isolated [BO₂(OH)] triangular groups to form a three-dimensional structure (Fig. 3a). Each [CaO₆] octahedron shares its four edges with neighboring octahedra in a double chain running along the **a** axis (Fig. 3b). Each planar [BO₂(OH)] group, which is parallel to (100), is linked to three [CaO₆] double chains simultaneously.

Miura & Kusachi (2008) carried out their Rietveld refinement by locating the B atom at the center of the BO₃ triangles and restricting the B–O bond distances to less than 1.40 Å, making the three B–O bond distances approximately equal (Table 4). Our single-crystal structure refinement shows that the B–OH bond distance, 1.412(4) Å, is significantly longer than the two B–O bonds, 1.356(4) and 1.365(4) Å (Table 4). This B–OH distance [see also 1.417(3) Å in parasibirskite] is significantly longer than the maximum B–O distance, 1.403 Å, for BO₃ triangles in borate minerals (Hawthorne *et al.* 1996). Similar B–OH distances have been obtained from periodic DFT calculations of sibirskite and parasibirskite at 0 K (Table 4). To the best of our knowledge, the isolated [BO₂(OH)] group in sibirskite (and parasibirskite) is new to nesoborate minerals (Hawthorne *et al.* 1996), although synthetic nesoborates consisting

TABLE 6. HYDROGEN BOND DISTANCES (Å) AND ANGLES (°) IN SIBIRSKITE, PARASIBIRSKITE, AND PRICEITE

D—H...A	d(D—H)	(H...A)	d(D...A)	<DHA
sibirskite (295 K)				
O(3)—H(1)...O(2)	0.84(4)	1.79(4)	2.619(3)	169(4)
parasibirskite (295 K)				
O(1)—H(1)...O(1)	0.97(2)	2.06(4)	2.8827(15)	142(4)
O(1)—H(1)...O(2)	0.97(2)	2.26(3)	3.140(2)	150(5)
parasibirskite (173 K)				
O(1)—H(1)...O(1)	0.97(2)	1.93(2)	2.878(2)	164(6)
O(1)—H(1)...O(2)	0.97(2)	2.42(5)	3.133(2)	130(5)
priceite (173 K)				
O(11)—H(1)...O(1)	0.85(3)	2.20(3)	3.007(4)	160(4)
O(10)—H(2)...O(1)	0.90(2)	1.97(2)	2.758(3)	145(4)
O(2)—H(3)...O(8)	0.92(2)	2.32(3)	2.917(3)	122(4)
O(5)—H(4)...O(10)	0.92(2)	1.79(2)	2.676(4)	160(4)
O(5)—H(4)...O(9)	0.92(2)	2.42(2)	3.121(3)	133(4)
O(6)—H(5)...O(4)	0.91(3)	1.85(3)	2.736(4)	163(4)
O(6)—H(5)...O(2)	0.85(3)	2.25(3)	3.088(4)	169(4)
OW(1)—H(6)...O(2)	0.87(3)	2.11(3)	2.977(4)	179(4)
OW(1)—H(7)...O(11)	0.87(3)	2.55(2)	3.059(4)	118(4)
OW(1)—H(7)...O(12)	0.85(3)	2.20(3)	3.007(4)	160(4)

D and A denote the hydrogen-bond "donor" and "acceptor", respectively.

of isolated $[\text{BO}_2(\text{OH})]$ groups are known (Menchetti & Sabelli 1982, Yu *et al.* 2002). For example, the isolated $[\text{BO}_2(\text{OH})]$ group in synthetic $\text{Na}_2[\text{BO}_2(\text{OH})]$ is also composed of a long B—OH bond of 1.439(3) Å and two short B—O bonds, 1.351(3) and 1.354(3) Å (Menchetti & Sabelli 1982). The three oxygen atoms, O(1), O(2) and O(3), of the $[\text{BO}_2(\text{OH})]$ group are linked to three, two and one Ca atoms, respectively (Fig. 3c).

The range of the Ca—O bond distances, from 2.316(2) to 2.407(2) Å (Table 4), is significantly smaller than that [2.302(4) to 2.426(4) Å] obtained from the Rietveld refinement of Miura & Kusachi (2008). Our single-crystal structure refinement also supports the hydrogen location on the O(3) atom suggested by Miura & Kusachi (2008). However, the experimental O—H bond distance of 0.84(4) Å is shorter than those (1.03 and 1.02 Å) inferred from bond-valence calculations (Miura & Kusachi 2008) and periodic DFT calculation at 0 K (Table 4). This difference arises from the fact that X-ray-diffraction experiments locate the center of the electron density, not the position of the nucleus as is used in bond-valence calculations.

The crystal structure of parasibirskite

Our single-crystal structure refinements of parasibirskite datasets measured at 173 and 295 K confirm the main structural features reported by Takahashi *et al.* (2010). The crystal structure of parasibirskite can

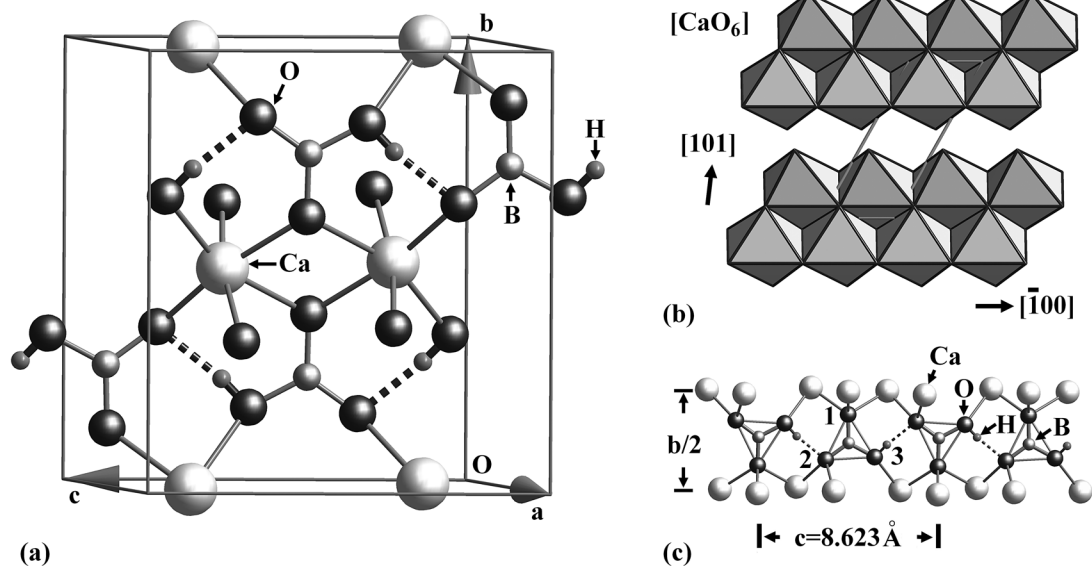


FIG. 3. The crystal structure of sibirskite: (a) unit cell, (b) the double chains of $[\text{CaO}_6]$ octahedra along the a axis, and (c) $[\text{BO}_2(\text{OH})]$ groups "linked" by hydrogen bonds to form a chain extending along the c axis, note that O(1), O(2) and O(3) are linked to three, two, and one Ca atom(s), respectively.

be described as sets of opposite edge-sharing $[\text{CaO}_7]$ chains along the c axis, which are linked together to form a corrugated layer parallel to (100). These $[\text{CaO}_7]$ layers are linked by the $[\text{BO}_2(\text{OH})]$ groups to form a three-dimensional structure (Figs. 4a, b).

The $[\text{CaO}_7]$ polyhedron in parasibirskite can be considered to be derived from the $[\text{CaO}_6]$ octahedron in sibirskite, where six O atoms are connected to one $[\text{BO}_2(\text{OH})]$ group each, and the seventh O atom is also linked to one of the six $[\text{BO}_2(\text{OH})]$ groups (Fig. 4a). The mean Ca–O distance, 2.421 Å (Table 4), is similar to that reported by Takahashi *et al.* (2010). However, the $[\text{BO}_2(\text{OH})]$ group reported by Takahashi *et al.* (2010) has one short B–O bond, 1.350(8) Å, and two long B–O bonds, 1.395(5) Å, with the former inferred to be the B–OH bond. Our refinement shows that the $[\text{BO}_2(\text{OH})]$ group in parasibirskite consists of two short B–O bonds, 1.349(2) Å and one long B–OH bond, 1.417(3) Å (Table 4).

Hydrogen atoms in the space group $P2_1/m$ at 295 K occur in a disordered mode, with 50% occupancies. In comparison, parasibirskite at 173 K has similar atomic positions, except that the hydrogen position is significantly different (Table 2). Specifically, two hydrogen-bond acceptors are located at 1.93 and 2.42 Å at 173 K, but at 2.06 and 2.26 Å at 295 K (Fig. 4c). Consequently, the d_{12} value in Figure 4c increases from

1.41 Å at 295 K to 1.70 Å at 173 K, whereas the d_{23} value decreases from 1.42 Å at 295 K to 1.03 Å at 173 K. These results suggest that parasibirskite may undergo a displacive phase-transition to the acentric space-group $P2_1$ involving hydrogen ordering below 173 K (Fig. 4d). This suggestion is supported by periodic DFT calculations for the space group $P2_1$ at 0 K (Table 4).

Therefore, sibirskite and parasibirskite, dimorphs of CaHBO_3 , are both nesoborates but differ in the modes of the isolated $[\text{BO}_2(\text{OH})]$ groups and the Ca polyhedra (*i.e.*, CN = 6 and 7, respectively). The $[\text{BO}_2(\text{OH})]$ groups in sibirskite are linked by hydrogen bonds to form a “chain” along the c axis (Fig. 3c), whereas those in parasibirskite are linked by hydrogen bonds to form a “ribbon” along the b axis (Fig. 4c).

The crystal structure of priceite

Our single-crystal structural refinement also confirms the structural model of priceite reported by Wallwork *et al.* (2002). Briefly, the crystal structure of priceite consists of the FBB $\{\text{B}_5\text{O}_7(\text{OH})_5\}^{4-}$, in which the central $[\text{BO}_4]$ tetrahedron shares two O corners with two $[\text{BO}_2(\text{OH})_2]$ tetrahedral groups, one O corner with a $[\text{BO}_3(\text{OH})]$ tetrahedral group, and the fourth O corner with a $[\text{BO}_3]$ planar triangular group (Fig. 5). This FBB, which can be labeled as $\Delta 4\Box<3\Box><\Delta 2\Box>$

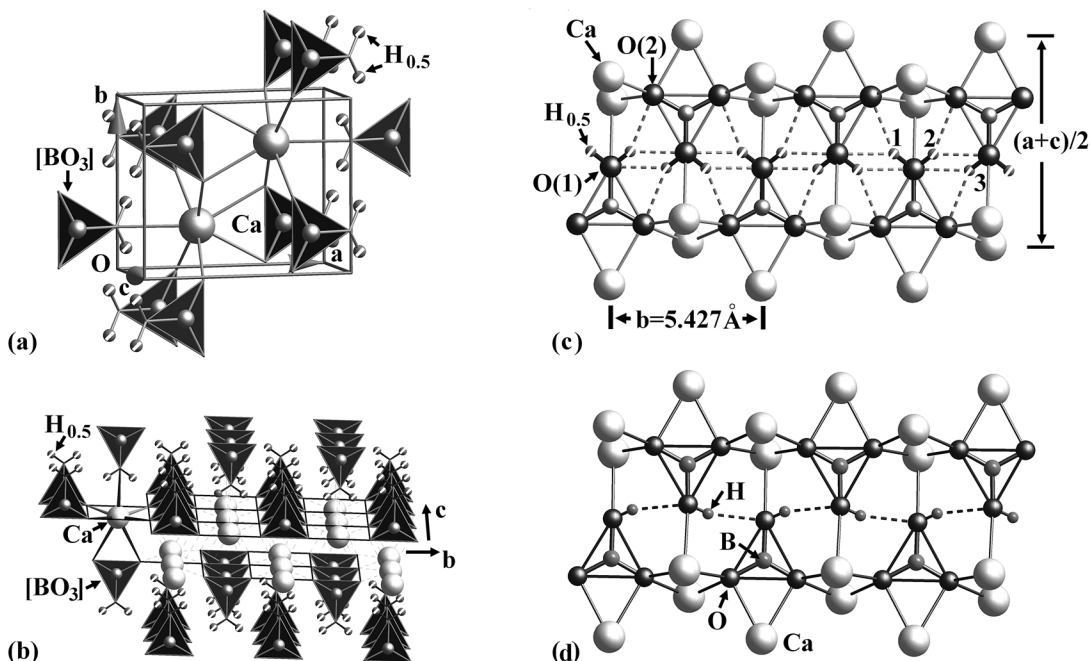


FIG. 4. The crystal structure of parasibirskite: (a) unit cell, (b) layers parallel to (100); (c) $[\text{BO}_2(\text{OH})]$ groups “linked” by hydrogen bonds to form a “ribbon” running along the b axis; note that three hydrogen atoms are marked 1, 2 and 3. (d) $[\text{BO}_2(\text{OH})]$ groups and $[\text{CaO}_7]$ groups in the space group $P2_1$ for comparison with those in (c).

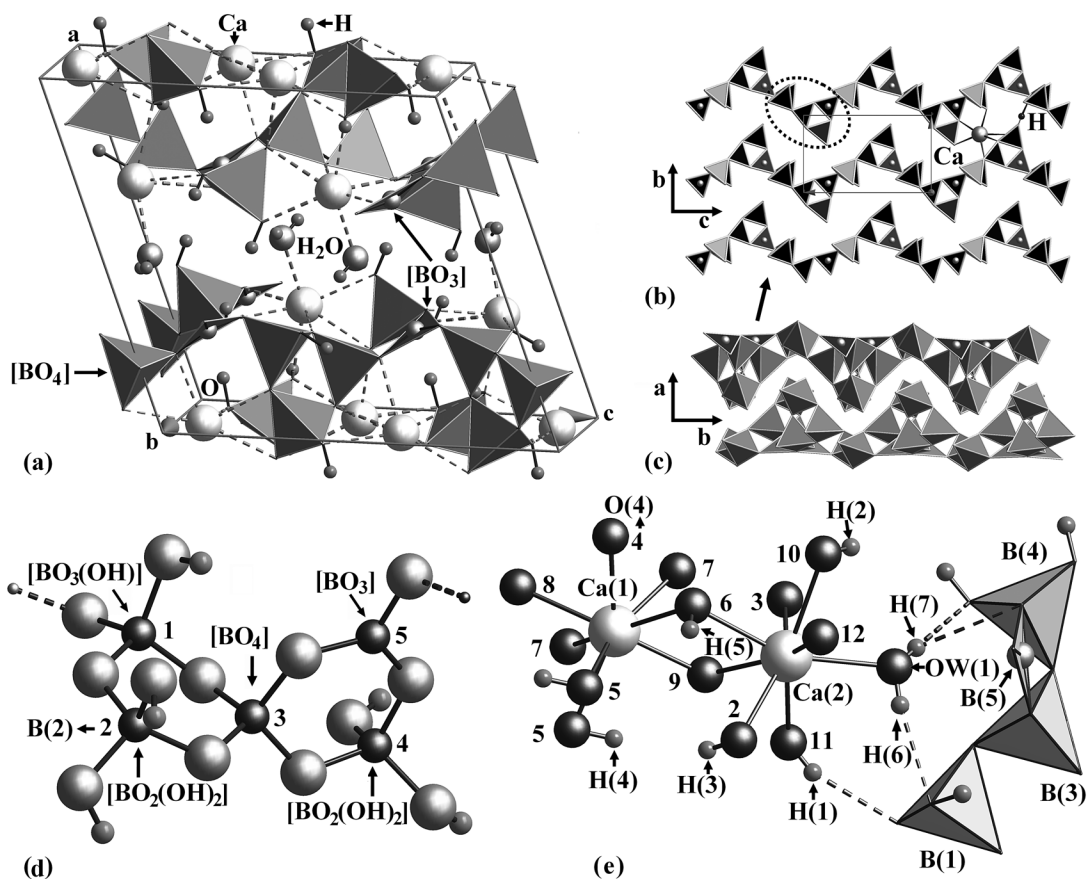


FIG. 5. The crystal structure of priceite. (a) Unit cell. (b) Zigzag chains of the FBB $\{B_5O_7(OH)_5\}^{4-}$ along the *c* axis. (c) Sawtooth-shaped sheets parallel to (100). (d) The FBB $\{B_5O_7(OH)_5\}^{4-}$. Note that the boron atoms and their coordination environment are marked. (e) Ca coordination environments, and hydrogen bonds are marked by dashed lines.

(Burns *et al.* 1995), contains two three-membered rings connected by the central [BO₄] tetrahedron, and links each other to form a zigzag infinite chain along the *c* axis. These chains are connected to each other by the Ca atoms and hydrogen bonds, and a backbone projection of these chains forms a sawtooth-shaped sheet parallel to (100), resulting from overlap of the infinite chains by viewing along the *c*-axis direction (Fig. 5b).

Two opposite sawtooth-shaped sheets chelate together *via* hydrogen bonds to form a thick layer parallel to (100) (Fig. 5c). These layers are connected by hydrogen bonds: one O(11)–H(1)...O(1) formed *via* the hydroxyl group and three OW(1)–H(6)...O(2), OW(1)–H(7)...O(11) and OW(1)–H(7)...O(12) formed *via* H₂O molecules (Table 6, Fig. 5e). The H₂O groups are located between the layers and coordinated with Ca atoms. The mean Ca–O bond distances of the two distinct 8-coordinated Ca sites are 2.471 Å and 2.454

Å, respectively (Table 5), similar to those reported by Takahashi *et al.* (2010). Our structure refinement provides accurate B–O bond distances and linkages involving the five distinct B sites in priceite (Table 5; Fleet & Muthupari 2000, Wallwork *et al.* 2002), adding to our knowledge about FBBs in borates (Hawthorne *et al.* 1996, Grice *et al.* 1999, Filatov & Bubnova 2000).

Stability of sibirskite and parasibirskite

Lehmann *et al.* (1958) reported the synthesis of parasibirskite from evaporation of an aqueous solution of Ca(OH)₂ and H₃BO₃ at pH = 12. Similarly, the XRD patterns of synthetic CaHBO₃ from the system Ca(OH)₂–H₃BO₃ at temperatures from 200 to 400°C (Hart & Brown 1962) and from 100 and 300°C (Schäfer 1968) are similar to that of parasibirskite (Kusachi *et al.* 1998). In addition, Liu *et al.* (2004) reported the

synthesis of parasibirskite from the mixture of CaO, H₃BO₃ and H₂O at 180°C. Our experiments support results of these earlier studies and show that parasibirskite can be synthesized over a wide range of conditions in basic solutions. On the other hand, sibirskite has never been synthesized before and appears to require more specific conditions, such as temperature, pressure, pH and impurity elements (*e.g.*, Cl).

Schindler & Hawthorne (2001a, 2001b, 2001c) proposed a pH–log[H₂O] diagram for borates and suggested that, with increasing activity of H₂O, the stable structural units change from frameworks to sheets, chains, clusters, and isolated polyhedra. Similarly, Ingri (1963) showed that the aqueous species [B(OH)₃]⁰ and [B(OH)₄][–] are stable at low pH and high pH, respectively, and borates formed under those conditions consist of triangular [Bφ₃] and tetrahedral [Bφ₄] groups. Schindler & Hawthorne (2001c) also pointed out that the ¹⁴B/(¹³B + ¹⁴B) value in borates increases with increasing pH and approaches 1.0 at pH ≥ 11. Therefore, the synthesis of parasibirskite and sibirskite, both of which contain an isolated [Bφ₃] group at pH ≈ 14 appears to be an exception to this rule. Admittedly, it is impossible to demonstrate that equilibrium, which is required for application of the pH–log[H₂O] diagram of Schindler & Hawthorne (2001a, 2001b, 2001c), was attained in our synthesis experiments.

Finally, it is interesting to note that our synthetic sibirskite and parasibirskite left in their parental solutions in air at ambient conditions decompose completely to form calcite (Fig. 2c) within one week. This result suggests that sibirskite and parasibirskite are not stable in basic solutions at ambient conditions.

ACKNOWLEDGEMENTS

We thank Drs. J.D. Grice, R.F. Martin, and Hexiong Yang for constructive reviews and helpful suggestions, National Natural Science Foundation of China (No. 40972035), Natural Science Foundation of Fujian Province (2010J01308) at the Scientific and Technological Innovation Platform of Fujian Province (2009J1009), and Natural Sciences and Engineering Research Council of Canada for financial support. The XRD datasets described in this paper were measured at the State Key Lab for Physical Chemistry of Solid Surfaces at Xiamen University.

REFERENCES

- BURNS, P.C., GRICE, J.D. & HAWTHORNE, F.C. (1995): Borate minerals. I. Polyhedral clusters and fundamental building blocks. *Can. Mineral.* **33**, 1131–1151.
- CHEN, C.T., WU, B.C., JIANG, A.D. & YOU, G.M. (1985): A new-type ultraviolet SHG crystal – β-BaB₂O₄. *Sci. Sinica, Ser. B* **28**, 235–243.
- DOVESI, R., SAUNDERS, V.R., ROETTI, C., ORLANDO, R., ZICOVICH-WILSON, C.M., PASCALE, F., CIVALLERI, B., DOLL, K., HARRISON, N.M., BUSH, I.J., D'ARCO, P. & LLUNELL, M. (2006): CRYSTAL06 User's Manual, University of Torino, Torino, Italy. <http://www.crystal.unito.it/manuals/crystal06.pdf>
- FILATOV, S.K. & BUBNOVA, R.S. (2000): Borate crystal chemistry. *Phys. Chem. Glasses* **41**, 216–224.
- FILATOV, S.K. & BUBNOVA, R.S. (2008): Structural mineralogy of borates as perspective materials for technological applications. *Minerals Adv. Mater.* **1**, 111–115.
- FLEET, M.E. & MUTHUPARI, S. (2000): Boron K-edge XANES of borates and borosilicates. *Am. Mineral.* **85**, 1009–1021.
- GATTI, C., SAUNDERS, V.R. & ROETTI, C. (1994): Crystal-field effects on the topological properties of the electron-density in molecular-crystals. The case of urea. *J. Chem. Phys.* **101**, 10686–10696.
- GRICE, J.D., BURNS, P.C. & HAWTHORNE, F.C. (1999): Borate minerals. II. A hierarchy of structures based upon the borate fundamental building block. *Can. Mineral.* **37**, 731–762.
- HART, P.B. & BROWN, C.S. (1962): The synthesis of new calcium borate compounds by hydrothermal methods. *J. Inorg. Nucl. Chem.* **24**, 1057–1065.
- HAWTHORNE, F.C., BURNS, P.C. & GRICE, J.D. (1996): The crystal chemistry of boron. In *Boron: Mineralogy, Petrology and Geochemistry* (E.S. Grew & L.M. Anovitz, eds.). *Rev. Mineral.* **33**, 41–115.
- INGRI, N. (1963): Equilibrium studies of polyanions containing B^{III}, Si^{IV}, Ge^{IV} and V^V. *Svensk Kem. Tidskr.* **75**, 3–34.
- KUSACHI, I., HENMI, C. & KOBAYASHI, S. (1997): Sibirskite from Fuka, Okayama Prefecture, Japan. *Mineral. J.* **19**, 109–114.
- KUSACHI, I., TAKECHI, Y., HENMI, C. & KOBAYASHI, S. (1998): Parasibirskite, a new mineral from Fuka, Okayama Prefecture, Japan. *Mineral. Mag.* **62**, 521–525.
- LEHMANN, H.-A., ZIELFELDER, A. & HERZOG, G. (1958): Zur Chemie und Konstitution borsaurer Salze. I. Die Hydrogenmonoborate des Calciums. *Z. Anorg. Allg. Chem.* **296**, 199–207.
- LIU, Z.H., ZUO, C.F. & LI, S.Y. (2004): Synthesis and thermochemistry of 2CaO•B₂O₃•H₂O. *Thermochim. Acta* **424**, 59–62.
- MENCHETTI, S. & SABELLI, C. (1982): Structure of hydrated sodium borate Na₂[BO₂(OH)]. *Acta Crystallogr.* **B38**, 1282–1285.
- MIURA, H. & KUSACHI, I. (2008): Crystal structure of sibirskite (CaHBO₃) by Monte Carlo simulation and Rietveld refinement. *J. Mineral. Petrol. Sci.* **103**, 156–160.

- PALACHE, C., BERMAN, H. & FRONDEL, C. (1951): *Dana's System of Mineralogy* (7th ed.). John Wiley & Sons, New York, N.Y.
- SCHÄFER, U.L. (1968): Synthese und röntgenographische Untersuchung der Borate $3\text{CaO}\cdot\text{B}_2\text{O}_3$, $2\text{CaO}\cdot\text{B}_2\text{O}_3$ und $2\text{CaO}\cdot\text{B}_2\text{O}_3\cdot\text{H}_2\text{O}$. *Neues Jahrb. Mineral., Monatsh.*, 75-78.
- SCHINDLER, M. & HAWTHORNE, F.C. (2001a): A bond-valence approach to the structure, chemistry and paragenesis of hydroxy-hydrated oxysalt minerals. I. Theory. *Can. Mineral.* **39**, 1225-1242.
- SCHINDLER, M. & HAWTHORNE, F.C. (2001b): A bond-valence approach to the structure, chemistry and paragenesis of hydroxy-hydrated oxysalt minerals. II. Crystal structure and chemical composition of borate minerals. *Can. Mineral.* **39**, 1243-1256.
- SCHINDLER, M. & HAWTHORNE, F.C. (2001c): A bond-valence approach to the structure, chemistry and paragenesis of hydroxy-hydrated oxysalt minerals. III. Paragenesis of borate minerals. *Can. Mineral.* **39**, 1257-1274.
- SHELDRIK, G.M. (1997): *SHELXS-97 and SHELXL-97[CP]*. University of Göttingen, Göttingen, Germany.
- SOLNTSEV, V.P., MASHKOVTSSEV, R.I., DAVYDOV, A.V. & TSVETKOV, E.G. (2008): EPR study of coordination of Ag and Pb cations in BaB_2O_4 crystals and barium borate glasses. *Phys. Chem. Minerals* **35**, 311-320.
- SPEK, A.L. (2003): Single-crystal structure validation with the program PLATON. *J. Appl. Crystallogr.* **36**, 7-13.
- SUN HUA-YU, SUN WEI, HUANG YA-XI & MI JIN-XIAO (2010): Low temperature flux synthesis and characterizations of a new layered barium borate $\text{BaB}_8\text{O}_{11}(\text{OH})_4$. *Z. Anorg. Allg. Chem.* **636**, 977-981.
- TAKAHASHI, R., KUSACHI, I. & MIURA, H. (2010): Crystal structure of parasibirskite (CaHBO_3) and polymorphism in sibirskite and parasibirskite. *J. Mineral. Petrol. Sci.* **105**, 70-73.
- VALENZANO, L., TORRES, F.J., DOLL, K., PASCALE, F., ZICOVICH-WILSON, C.M. & DOVESI, R. (2006): *Ab initio* study of the vibrational spectrum and related properties of crystalline compounds; the case of CaCO_3 calcite. *Z. Phys. Chem.* **220**, 893-912.
- VASILKOVA, N.N. (1962): A new calcium borate, sibirskite. *Zap. Vser. Mineral. Obshchest.* **91**, 455-464 (in Russian).
- WALLWORK, K.S., PRING, A., TAYLOR, M.R. & HUNTER, B.A. (2002): The structure of priceite, a basic hydrated calcium borate, by *ab initio* powder-diffraction methods. *Can. Mineral.* **40**, 1199-1206.
- WEIGEND, F. & AHLRICHS, R. (2005): Balanced basis sets of split valence, triple zeta valence and quadruple zeta valence quality for H to Rn: design and assessment of accuracy. *Phys. Chem. Chem. Phys.* **7**, 3297-3305.
- YU, Z.-T., SHI, Z., CHEN, W., JIANG, Y.-S., YUAN, H.-M. & CHEN, J.-S. (2002): Synthesis and X-ray crystal structures of two new alkaline-earth metal borates: $\text{SrBO}_2(\text{OH})$ and $\text{Ba}_3\text{B}_6\text{O}_9(\text{OH})_6$. *J. Chem. Soc., Dalton Trans.*, 2031-2035.
- YUAN, G. & XUE, D. (2007): Crystal chemistry of borates: the classification and algebraic description by topological type of fundamental building blocks. *Acta Crystallogr.* **B63**, 353-362.

Received December 11, 2010, revised manuscript accepted May 12, 2011.